Available online at www.sciencedirect.com
SCIENCE DIRECT®
Microelectronic Engineering 83 (2006) 1814–1817
MICROELECTRONIC ENGINEERING
www.elsevier.com/locate/mee

Strategies for integration of donor electron spin qubits in silicon

T. Schenkel [a], J.A. Liddle [a], J. Bokor [a,b,c], A. Persaud [a], S.J. Park [a], J. Shangkuan [a,b], C.C. Lo [b], S. Kwon [c], S.A. Lyon [d], A.M. Tyryshkin [d], I.W. Rangelow [e], Y. Sarov [e], D.H. Schneider [f], J. Ager [a], R. de Sousa [g,*]

[a] *E.O. Lawrence Berkeley National Laboratory, Berkeley, CA 94720, USA*
[b] *Department of Electrical Engineering and Computer Science, University of California, Berkeley, Ca 94720, USA*
[c] *The Molecular Foundry, Lawrence Berkeley National Laboratory, Berkeley, Ca 94720, USA*
[d] *Department of Electrical Engineering, Princeton University, Princeton, NJ 08544, USA*
[e] *Institute of Microstructure Technologies and Analytics, University of Kassel, Germany*
[f] *Lawrence Livermore National Laboratory, Livermore, CA 94550, USA*
[g] *Department of Chemistry and Pfizer Center for Theoretical Chemistry, University of California, Berkeley, CA 94720, USA*

Available online 2 March 2006

Abstract

Spins of electrons bound to donor electrons are attractive candidates for exploration of quantum information processing in silicon. We present results from our development of donor electron spin qubit structures. Donors are placed into isotopically enriched ^{28}Si by ion implantation. The coherence properties of donor implants in pre-device structures are probed by pulsed electron spin resonance (ESR). The spin de-coherence time, T_2, for ^{121}Sb donors implanted into a peak depth of 50 nm from a thermal oxide interface is 0.3 ms at 5 K, increasing to 0.75 ms when the silicon surface is passivated with hydrogen. A technique for formation of donor arrays by ion implantation with scanning force microscope alignment is presented, and we discuss coherence limiting factors with respect to the implementation of a single spin readout scheme.
Published by Elsevier B.V.

PACS: 03.67.Lx; 07.79.Lh; 73.23.Hk; 85.35.Gv; 81.16.Nd; 73.22.Dj

Keywords: Quantum computing; Electron spin resonance; Ion implantation; Single electron transistor

1. Introduction

Quantum computation [1] promises to revolutionize information technology, and there is currently intense interest in identifying quantum bit (qubit) systems that allow realization of computational tasks beyond the reach of conventional computers. Spins of electrons [2,3] and nuclei [4] of single donor atoms placed into arrays in a silicon matrix are attractive qubit candidates due to their long coherence times [5], and the fabrication finesse of silicon based nanoelectronics. In this article we present results from studies of donor electron spins in ion -implanted silicon, we describe a single ion placement technique, and we discuss requirements for a readout device for detection of single donor electron spins.

2. Ion implantation and annealing

Ion implantation is a standard technique for introduction of dopants into semiconductors. It is accompanied by damage to the host material and a high temperature anneal is required to remove this damage and to move implanted atoms to lattice positions where they are electrically active. It is not obvious that the high degree of perfection required for a quantum computer is compatible with ion implantation. In addition, long coherence times of up

* Corresponding author. Tel.: +001 510 486 6674; fax: +001 510 486 5105.
E-mail address: T_Schenkel@LBL.gov (R. de Sousa).

0167-9317/$ - see front matter. Published by Elsevier B.V.
doi:10.1016/j.mee.2006.01.234

to 60 ms were previously demonstrated only for bulk doped samples. Integration into devices requires placement of dopant arrays close to imperfect interfaces.

We implanted isotopically enriched ^{28}Si epi-wafers (500 ppm residual ^{29}Si content) with a low dose of ^{121}Sb ions. The implant energy was 120 keV, and the dose was 2×10^{11} cm^{-2}. Sb was chosen as a donor element to avoid any ambiguity of ESR signals from a phosphorus (P) background contamination of order 3×10^{13} cm^{-3} in the starting material. In addition, the scattering kinematics favours placement of heavy donors into silicon, leading to lower straggling for Sb compared to P implants into a given depth. The first task is the electrical activation and damage repair by rapid thermal annealing. Fig. 1 shows a secondary ion mass spectrometry depth profile of the Sb implant after RTA (1000 °C, 10 s, N_2/H_2) together with spreading resistance analysis data, and a dynamical Monte Carlo simulation of the as-implanted depth profile. SIMS profiles of the as-implanted samples are currently not available, but the simulations have been found to be very accurate in previous studies [6]. The SIMS data agree very well with the simulation. The very limited symmetrical broadening indicates a very low level of diffusion during RTA.

The apparent electrical activation was found to be only 3.4% in spreading resistance analysis (SRA) measurements, but we have observed that standard SRA is of limited utility for the present low carrier concentrations relatively close to the sample surface. Sample illumination during ESR measurements led to significantly increased spin counts, indicating that donors are to a high degree incorporated into the lattice substitutionally. But a large fraction of donors appears to be ionized due to band bending at the ungated interface. We point out that the dopant movement is significantly less for antimony compared to low dose phosphorous implants in the presence of an SiO_2/Si interface [7]. This is consistent with the different diffusion mechanisms for these two donors. Phosphorus diffuses through an interstitial mechanism, and thus couples to interstitials that are injected from the SiO_2/Si interface during annealing, which leads to the pile up of phosphorous at the interface. Antimony is a vacancy diffuser, and dopant movement is retarded by injection of interstitials.

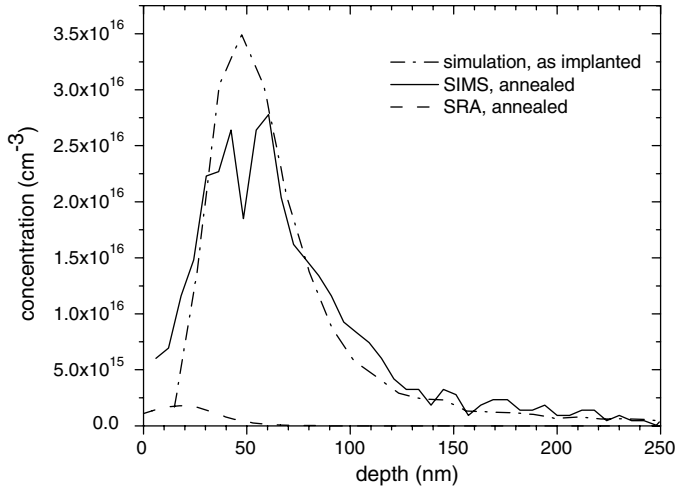

Fig. 1. SIMS and SRA data and Monte Carlo simulation of ^{121}Sb implant (120 keV) depth profile.

3. Electron spin resonance of implanted donors

We probe donor electron spin coherence by pulsed ESR [5] with an x-band spectrometer at 5 K. Fig. 2 shows a typical spectrum from ^{121}Sb donors in a ^{28}Si sample. The removal of the ^{29}Si isotopes results in remarkably narrow line widths of about 60 mG for the six hyperfine split resonant lines. The broad feature in the center is from defects due to sample preparation.

In order to see the effect of ion implantation and annealing we compared the ESR spectra from implanted ^{121}Sb donors to the spectra from phosphorous donors that were present as a low concentration background doping in a 25 μm thick epi-layer (^{31}P doping of 10^{15} cm^{-3}) and in a pure ^{28}Si crystal (P concentration 3.5×10^{14} cm^{-3}) [8]. The different hyperfine coupling strengths of ^{121}Sb and ^{31}P required a scaling of the magnetic field axis to allow the direct comparison shown in Fig. 3. The comparison reveals a slight broadening of the spin resonance lines already for the 25 μm thick epi-layer in comparison to the ^{28}Si crystal. This is a result of imperfect epitaxial

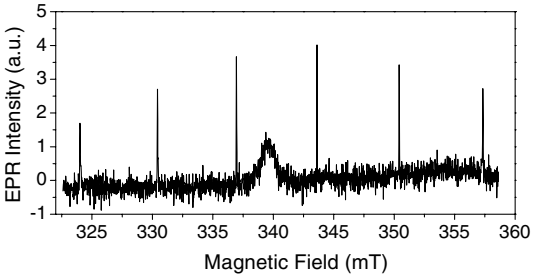

Fig. 2. x-band ESR spectrum of ^{121}Sb donors in implanted ^{28}Si epi layer at 5 K.

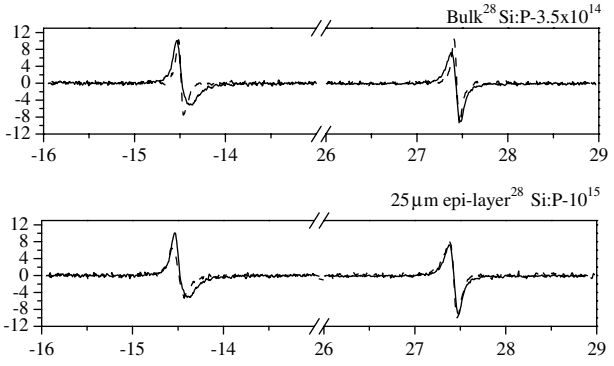

Fig. 3. Comparison of the ±5/2 lines of ^{121}Sb donors (solid curves) in an implanted and annealed epi-layer to ^{31}P lines (dashed curves) from background doping of (top) a in a ^{28}Si crystal, and (bottom) a ^{28}Si epi-layer.

growth and the build-up of stress. T_2 was 4 ms for the phosphorus in the ^{28}Si crystal at 5 K, probably limited by instantaneous diffusion [5]. Ion implantation results also in a slight broadening, but resonance lines remain very narrow, and the effect of any residual defects from incomplete damage repair as well as the effect of the SiO_2/Si interface are minimal. The donor electron spin coherence time was evaluated by Hahn spin echo decay measurements [3] and we found a T_2 time of 0.3 ms for the low dose, 120 keV ^{121}Sb implants at 5 K. Increasing the average depth of implanted donors to 150 nm by implantation with 400 keV increased T_2 to 1.5 ms. Passivation of the silicon surface with hydrogen (through a standard dip in a hydrofluoric acid solution) increased T_2 from 0.3 ms to 0.7 ms for 120 keV implants, and from 1.5 ms to 2.1 ms for 400 keV implants [6]. This increase of T_2 demonstrates that defects (e.g., dangling bonds and trapped charges) in the oxide and at the SiO_2/Si interface limit T_2 for shallow implants and show that hydrogen passivation is a promising method for retention of long T_2 times. The thermal oxide used here had interface and trapped charge densities of about 2×10^{11} cm^{-2}, over an order of magnitude more then achievable with optimized processing.

4. Ion placement with scanning probe alignment

Testing of donor qubits will require formation of single donor arrays. One method for qubit array formation is single ion implantation. We have developed an instrument in which an ion beam is aligned to sample features with a scanning force microscope (SFM) [9]. Here, ions are transported through a hole in the tip of a piezoresistive force sensor. SFM imaging is non-destructive and no ions reach the sample during imaging. The latter is an obstacle to single atom array formation with Focused Ion Beam systems [10]. Fig. 4 shows a schematic of the experimental setup.

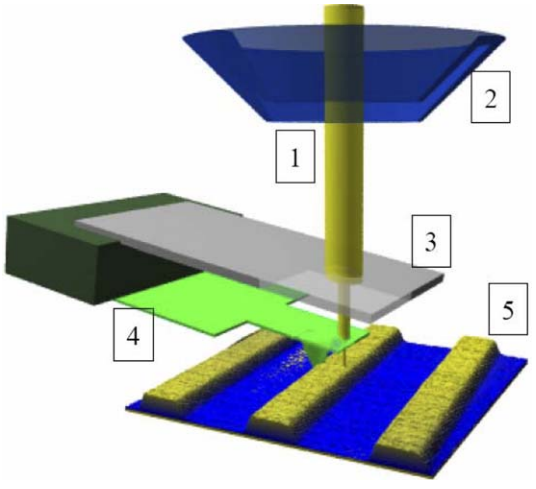

Fig. 4. Schematic of the setup for ion implantation with scanning probe alignment, showing the ion beam (1) transported though an electrostatic lens element (2) to a pre-collimating aperture (3) and the cantilever with final aperture (4). The image shows data from *in situ* imaging of 20 nm high, 1 μm wide metal lines with 3 μm spacing.

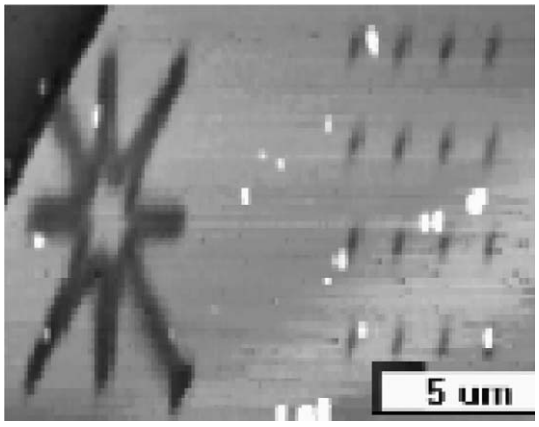

Fig. 5. Patterns formed by ion implantation with scanning probe alignment in PMMA on silicon.

With this instrument we have formed patterns in 30 nm thick poly-methyl-metacrylate (PMMA) layers on silicon (Fig. 5). The diameter of the final beam collimating aperture in the cantilever was about 100 nm for these patterns. The patterns were formed by exposure of the resist to 7 keV Ar^{2+} ions (dose about 10^{13} cm^{-2}). The dots in the 4×4 array are slightly elongated, probably due to drift in the sample stage. The current imaging and alignment resolution of the instrument is ~5 nm, sufficient for formation of single and few qubit test devices. The later will require integration of high-resolution ion placement with single ion detection capability, e.g., based on detection of secondary electrons [10,11] or collection of electron–hole pairs inside the sample in a silicon detector adaptation [12].

5. Development of a single spin readout transistor

A reliable single spin readout is necessary for demonstration of rudimentary control over spin states in donor electrons. One promising route to achieve this is based on spin dependent electron transfer between two donors and the sensing of a successful electron transfer with a single electron transistor [13]. Towards implementation of a single spin readout scheme, we have developed single electron transistors in silicon using an SOI (silicon on insulator) process [11,14]. An example of a pair of silicon nanowire SETs is shown in Fig. 6.

Electrical characterization at 4 K shows Coulomb blockade and gate modulation of the source-drain current (Fig. 7). The charging energy of the SETs with 15 nm wire width was about 6 meV. While formation of Coulomb blockade devices in silicon nanostructures is not controversial, it is not evident how tunnel junctions from the nanowire island to the highly doped source and drain leads are formed. We did not apply stress-limited oxidation due to direct access to 15 nm wire width by e-beam lithography and a bi-layer resist process [14]. Dopant segregation in the doped nanowires is a likely mechanism for tunnel

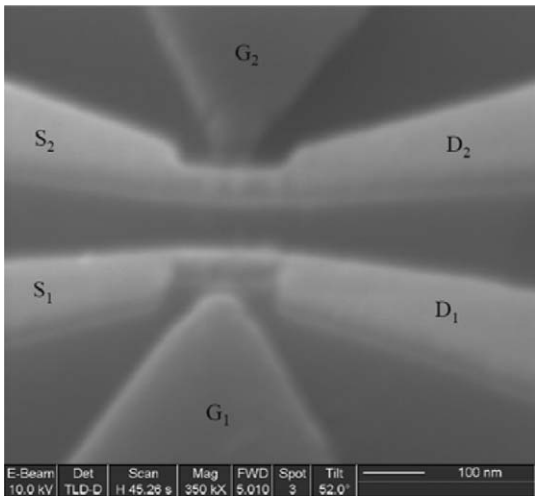

Fig. 6. Pair of single electron transistors formed in SOI.

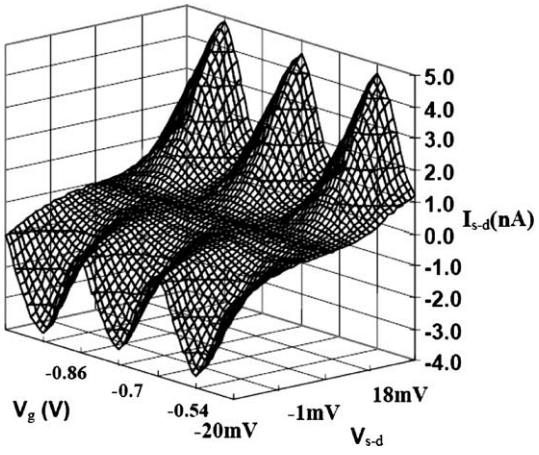

Fig. 7. Coulomb blockade (I_{sd} vs. V_{sd}) and gate modulation of the source-drain current in a silicon nanowire SET with a 15 nm wire width at 4.2 K.

junction formation, as are edge roughness and nanowire oxidation in thermal processing such as annealing of the source and drain implants.

With respect to the detrimental effect of a close SiO_2 interface on T_2, we note that the SOI architecture, which allows formation of silicon nanowires, is detrimental to long T_2 times. This effect can be mitigated by forming gas anneals that passivate dangling bonds and trapped charges in the oxides close to the donors. From the ESR studies we can expect T_2 times of about 0.3–1 ms for donors placed into 30 nm high silicon nanowires surrounded by oxide. The trap and defect dynamics (e.g., charging and discharging as well as spin flips in paramagnetic traps) is temperature dependent and we can thus expect longer T_2 times at lower temperatures. Due to the nuclear spin free environment, coherence times in isotopically enriched silicon (^{28}Si) are over two orders of magnitude longer then the longest coherence times observed for electron spins in GaAs based quantum dots [15]. We are hoping to soon reach levels of control at the single electron level that have been demonstrated in the latter.

6. Conclusion

Spins of electrons bound to donor atoms in silicon are promising candidates for the development of quantum computer test structures. In a top down approach, we show that ion implantation of donors into ^{28}Si samples is compatible with coherence times in excess of 1 ms at 5 K. Defects at the SiO_2/Si interface limit coherence for shallow implants, and much longer coherence times are expected at lower temperatures and for improved interfaces. We have developed a technique for formation of ion arrays where the ion beam is aligned with a scanning force microscope. Single spin readout devices, such as single electron transistor, or spin dependent transport transistors can now be implanted with single donor ions, enabling testing of quantum computer test structures with donor electron qubits.

Acknowledgments

This work was supported by NSA under ARO Contract No. MOD707501. Work at LBNL was supported by the U.S. DOE under Contract No. DE-AC02-05CH1123. Work at LLNL was supported by the U. S. DOE under Contract No. DE-AC03-76SF00098. Part of this work was supported by NSF under Grant No. 0404208. Work at Princeton was supported by ARO and ARDA under Contract No. DAAD19-02-1-0040.

References

[1] M.A. Nielson, I.L. Chuang, Quantum Computation and Quantum Information, Cambridge University Press, Cambridge, 2000.
[2] R. Vrijen et al., Phys. Rev. A 62 (2000) 12306.
[3] R. DeSousa, J.D. Delgado, S. Das Sarma, Phys. Rev. A 70 (2004) 052304.
[4] B.E. Kane, Nature 393 (1998) 133.
[5] A.M. Tyryshkin, S.A. Lyon, A.V. Astashkin, A.M. Raitsimring, Phys. Rev. B 68 (2003) 193207.
[6] T. Schenkel et al., cond-mat/0507318.
[7] A. Persaud et al., Quantum Info. Process. 3 (2004) 233.
[8] J.W. Ager et al., J. Electrochem. Soc. 152 (2005) G448.
[9] A. Persaud et al., NanoLetters 5 (2005) 1087.
[10] T. Shinada et al., Jpn. J. Appl. Phys. 41 (2002) L-287.
[11] S.J. Park et al., Microelectron. Eng. 73 (2004) 695.
[12] D.N. Jamieson et al., Appl. Phys. Lett. 86 (2005) 202101.
[13] B.E. Kane et al., Phys. Rev. B 61 (2000) 2961; T.M. Buehler et al., Appl. Phys. Lett. 86 (2005) 143117.
[14] S.J. Park et al., J. Vac. Sci. Technol. 22 (2004) 3115.
[15] J.R. Petta et al., Science 309 (2005) 2180.